

# Electrostatic solitary waves associated with magnetic anomalies and wake boundary of the Moon observed by KAGUYA

K. Hashimoto,<sup>1</sup> M. Hashitani,<sup>1</sup> Y. Kasahara,<sup>2</sup> Y. Omura,<sup>1</sup> M.N. Nishino,<sup>3</sup> Y. Saito,<sup>3</sup> S. Yokota,<sup>3</sup> T. Ono,<sup>4</sup> H. Tsunakawa,<sup>5</sup> H. Shibuya,<sup>6</sup> M. Matsushima,<sup>5</sup> H. Shimizu,<sup>7</sup> and F. Takahashi<sup>5</sup>

We present observations of electrostatic solitary waves (ESWs) near the Moon by SELENE (KAGUYA) in the solar wind and in the lunar wake. SELENE is a lunar orbiter with an altitude of 100km and measured wave electric field, background magnetic field, and fluxes of ions and electrons, etc. ESWs are categorized into three types depending on different regions of observations: ESWs generated by electrons reflected and accelerated by an electric field in the wake boundary (Type A), strong ESWs generated by bi-streaming electrons mirror-reflected over the magnetic anomaly (Type B), and ESWs generated by reflected electrons when the local magnetic field is connected to the lunar surface (Type C). ESWs of Type C often alternate with Langmuir waves.

## 1. Introduction

The discovery of electrostatic solitary waves (ESWs) [Matsumoto *et al.*, 1994] was a scientific milestone that had clarified that the main part of the broadband electrostatic noise (BEN) [Gurnett *et al.*, 1976] is a series of bipolar pulses corresponding to electron holes in the velocity phase space. They are generated by a bi-stream electron beam instability [Omura *et al.*, 1994] or a bump-on-tail instability driven by an electron beam in a warm thermal plasma [Omura *et al.*, 1996]. Since ESWs represent nonlinear electron dynamics associated with electron acceleration, they can be used as a diagnostic tool for nonthermal components of electron velocity distribution functions with time resolution much higher than those by direct particle measurements [Omura *et al.*, 1999]. ESWs have been observed on many other spacecraft, such as FAST, Polar, and WIND, in various regions of the magnetospheres such as plasma sheet boundary layer, bow shocks, and polar ionospheres.

The SELENE (KAGUYA) spacecraft was launched on September 14, 2007 as the first Japanese lunar exploration mission. It examined the distribution of elements and minerals on the surface, the surface and sub-surface structures, the gravity field, the magnetic field, and the plasma environment on and around the Moon. The Lunar Radar Sounder (LRS) [Ono *et al.*, 2008] is one of the scientific instruments onboard the KAGUYA main orbiter [KAGUYA (SELENE) website]. The LRS consists of three subsystems: SDR (SounDeR observation), NPW (Natural Plasma Wave receiver), and WFC (WaveForm Capture). The WFC is a software receiver [Hashimoto

*et al.*, 2003] in which most of the functions are realized by a digital signal processor (DSP) implemented on the WFC board and covers the frequency range from 100 Hz to 1 MHz. The main electronics of the WFC consists of two kinds of passive receivers named WFC-H and WFC-L [Kawahara *et al.*, 2008] connected to two orthogonal 30 m tip-to-tip antennas. The WFC-H is a fast sweep frequency analyzer covering the frequency range from 1 kHz to 1MHz. The WFC-L measures waveforms in the frequency range from 100 Hz to 100 kHz. Data used in the present paper were intermittently acquired with a duration of 1.5 seconds almost every 2 minutes. A comprehensive diagnosis of electromagnetic and plasma environment in the near-Moon space by means of in-situ measurements of electrons, ions, and magnetic field is performed onboard by MAP (MAGnetic field and Plasma experiment) / PACE (Plasma energy Angle and Composition Experiment) [Saito *et al.*, 2008] and MAP/LMAG (Lunar MAGnetometer) [Shimizu *et al.*, 2008; Takahashi *et al.*, 2009]. Based on the LMAG observations in the tail lobe and the lunar wake, global maps of lunar magnetic anomalies are obtained with 95 % coverage of the lunar surface [Tsunakawa *et al.*, 2010].

Ogilvie *et al.* [1996] reported new aspects including the plasma density decrease and the ion acceleration by an electric field when the Wind satellite crossed the lunar wake at a distance of 6.8 lunar radii in 1994. Kellogg *et al.* [1996] observed BEN and a series of waveforms in this period although no ESWs were reported.

## 2. Observations

KAGUYA took a polar orbit of the Moon at 100 km altitude with a 2-hour period. As a result of interaction between the solar wind and the Moon, the lunar wake is formed on the backside of the Moon. Figure 1(a) shows an example of waveforms observed at 0418 UT on April 2, 2008 at the wake boundary. The local electron density or plasma frequency at 0422 UT just after the observed time increased to about 0.16/cc or 3.6 kHz. Halekas *et al.* [2005] show electron density profiles in the wake region. The same type of bipolar pulses generated by an electron hole as those observed with GEOTAIL [Matsumoto *et al.*, 1994] is seen in the component parallel to the background magnetic field. Similar ESWs are observed in three different regions, generated in somewhat different ways in each region, and are classified into three types. Behind the Moon, lighter and faster electrons fill in the wake ahead of the ions. The resultant ambipolar electric field accelerates the ions to the cavity [Ogilvie *et al.*, 1996]. The electrons are accelerated in the counter-streaming direction to the solar wind. As a result of an electrostatic instability driven by the energetic particles, ESWs are generated [Omura *et al.*, 1996]. We call them Type A ESWs. The nadir angle, which is indicated as 'angle' in the figure, is defined as an angle between the background magnetic field and the downward direction opposite to the zenith.

Another example of ESWs observed in the solar wind over a magnetic anomaly [Hood *et al.*, 2001] on the sunlit side of the Moon is shown in Fig. 1(b). This figure shows electric field components observed on May 2, 2008. These ESWs are caused by electrons in the solar wind and the counter-streaming electrons mirror-reflected over the anomaly. We call them Type B ESWs. It should be noted that the time scales are different by a factor of five between Figures 1(a) and (b) because of the electron density

difference. The velocities of ESWs can be measured from the time difference between the two monopole antennas in the interferometry mode [Kasahara *et al.*, 2008] although results of this mode are not shown in the present paper because of the limited space. The velocities are much smaller at the wake boundary than those observed above magnetic anomalies in the dayside solar wind.

Figure 2 is a schematic illustration of the KAGUYA orbit. Along the blue dashed line behind the Moon, the wake electric field [Ogilvie *et al.*, 1996] is shown. This field plays an important role in generation of Type-A ESWs in the wake region, since the field accelerates electrons in the counter-streaming direction to the solar wind. A magnetic anomaly which plays another important role in generation of Type-B ESWs is also illustrated.

E-t (Energy-time) diagrams of particles by MAP/PACE, wave spectra by WFC-H, and magnetic fields by MAP/LMAG observed on February 6, 2008 in a wake boundary are shown in Figure 3. The tail angle is defined as the angle between the magnetic field direction and the X-axis (Sun-Moon direction) in the selenocentric solar ecliptic (SSE) coordinates. After 0300 UT at the wake boundary in the cyan blue zones, BENs (spiky emissions below 10 kHz in Figure 3(e)) are observed when the tail angle (green line in Figure 3(g)) is close to 0 degrees in this region, since the magnetic field is expected to be connected to the electric field in the wake far from the Moon [Ogilvie *et al.*, 1996]. Nadir angles are not important in this region. These BENs correspond to Type A ESWs. In addition to Type-A ESWs, so-called type-II proton entries [Nishino *et al.*, 2009] observed in the wake boundary are at times accompanied by ESWs [Nishino *et al.*, 2010].

Type B ESWs observed above magnetic anomalies on February 12, 2008 are shown in Figure 4 in the same format as that of Figure 3. Intense waves at 10-20 kHz in Figure 4(e) are Langmuir waves enhanced at the local plasma frequency  $f_p$ . Langmuir waves are generally observed in the sunlit region and boundaries facing the Sun and in the lunar wake while the Moon is in the solar wind. At a magnetic anomaly of about 1 nT around 1530 UT in the red zone, strong BENs are observed, which correspond to Type B ESWs. At the same time, fluxes of electrons and ions are enhanced especially in the Moon side ESA1 and IMA in Figures 4(b) and 4(d), respectively, because electrons are efficiently reflected at mirror points near the strong magnetic field of the lunar surface. Sometimes, as seen around 1545 UT, Langmuir waves are observed with wider bandwidths. Modulated electron plasma waves are observed in such times as reported by Kellogg *et al.* [1996]; Kojima *et al.* [1997].

Observations without a magnetic anomaly in the solar wind on May 6, 2008 are shown in Figure 5 in the same format as that of Figure 3. When the nadir angle is not close to 90 degrees as seen in Figure 5(g), that is, the magnetic field is connected to the lunar surface, Langmuir waves (emissions at the local plasma frequency near a few 10 kHz or lower) or BENs are excited. The BENs around 2040 UT correspond to ESW without any association to magnetic anomalies. We call them Type C ESWs.

### 3. Summary and Discussion

Three types of ESW observations near the Moon are reported. Type A ESWs are observed at the wake boundaries as shown in Figure 3. Type B ESWs are observed

above magnetic anomalies. Strong wave activities associated with enhancement of electron fluxes are observed above magnetic anomalies as shown around 1530 UT in Figure 4. Type C ESWs are observed in the solar wind above the moon surface without magnetic anomalies.

Considering that electron beams are necessary for ESW generation, we can reasonably assume the following scenario as the generation mechanism of the three types of ESWs.

1) Type A ESWs at the wake boundaries are generated far from the Moon. The energetic electrons accelerated by the strong electric field at the wake boundary move along the magnetic field line [Ogilvie *et al.*, 1996], resulting in the bump-on-tail instability. They propagate along the magnetic field to the KAGUYA orbits. A series of potentials due to the instability coalesce with each other to form larger and longer solitary potentials through propagation along the magnetic field. The longer distance of propagation in the wake boundary makes the amplitude of ESWs comparable to those due to the strong bi-stream instability occurring in the short distance above the day-side magnetic anomalies.

2) Type B ESWs are observed by KAGUYA when the magnetic fields are connected to the Moon with their nadir angles not close to 90 degrees. Because of the strong magnetic field near the Moon surface, a substantial amount of electrons are reflected at mirror points above the anomalies. Total field strengths of magnetic anomalies at the surface of the Moon as derived from the Lunar Prospector electron reflectometer experiment [Mitchell *et al.*, 2008] reach more than 40 nT.

3) Langmuir waves or ESWs are alternately observed in Type C ESW events. Since the electron reflection over the surface without magnetic anomalies is relatively weak, a weak beam is formed, resulting in the weak-beam instability or the bump-on tail instability. Either Langmuir waves or ESWs are generated depending on the background electron and ion thermal velocities [Omura *et al.*, 1996].

In the electron flux measurement, we find a clear correlation between electron flux increase and Type B ESW generation above the magnetic anomalies, while the electron beams generating Type A and C ESWs are too weak to be observed in the E-t diagrams. Detailed analysis of the particle data and exact identification of the plasma conditions for these ESWs are left as a future study.

**Acknowledgments.** The authors express their thanks to all members of the KAGUYA project team.

## References

- Gurnett, D. A., L. A. Frank, and R. P. Lepping (1976), Plasma waves in the distant magnetotail, *J. Geophys. Res.*, *81*, 6059
- Halekas, J. S., S. D. Bale, D. L. Mitchell, and R. P. Lin, Electrons and magnetic fields in the lunar plasma wake, *J. Geophys. Res.*, *110*, A07222, doi:10.1029/2004JA010991.
- Hashimoto, K., H. Iwai, Y. Ueda, H. Kojima, and H. Matsumoto (2003), Software wave receiver for the SS-520-2 rocket experiment, *IEEE Trans. on Geoscience and Remote Sensing*, *41*, 2638–2647.
- Hood, L. L., A. Zakharian, J. Halekas, D. L. Mitchell, R. P. Lin, M. H. Acuna, and A. B. Binder (2001), Initial mapping and interpretation of lunar crustal magnetic anomalies using Lunar Prospector magnetometer data, *J. Geophys. Res.*, *106*, 27825–27839.

- KAGUYA (SELENE) website,  
[http://www.jaxa.jp/projects/sat/selene/index\\_e.html](http://www.jaxa.jp/projects/sat/selene/index_e.html)
- Kasahara, Y., Y. Goto, K. Hashimoto, T. Imachi, A. Kumamoto, T. Ono, and H. Matsumoto (2008), Plasma Wave Observation Using Waveform Capture in the Lunar Radar Sounder on board the SELENE Spacecraft, *Earth, Planets and Space*, *60*, 341–351.
- Kellogg, P. J., K. Goetz, S. J. Monson, J.L. Bougeret, R. Manning, and M. L. Kaiser (1996), Observations of plasma waves during a traversal of the Moon’s wake, *Geophys. Res. Lett.*, *23*, 1267–1270.
- Kojima, H., H. Furuya, H. Usui, H. Matsumoto (1997), Modulated electron plasma waves observed in the tail lobe: Geotail waveform observations, *Geophys. Res. Lett.*, *24*, 3049–3052.
- Matsumoto, H., H. Kojima, T. Miyatake, Y. Omura, M. Okada, I. Nagano, and M. Tsutsui (1994), Electrostatic Solitary Waves (ESWs) in the Magnetotail: BEN Wave forms observed by GEOTAIL, *Geophys. Res. Lett.*, *21*, 2915–2918.
- Mitchell, D.L., J.S. Halekas, R.P. Lina, S. Freya, L.L. Hood, M.H. Acunad, A. Binder (2008), Global mapping of lunar crustal magnetic fields by Lunar Prospector, *Icarus*, *194*, 401–409.
- Nishino, M. N., M. Fujimoto, K. Maezawa, Y. Saito, S. Yokota, K. Asamura, T. Tanaka, H. Tsunakawa, M. Matsushima, F. Takahashi, T. Terasawa, H. Shibuya, and H. Shimizu (2009), Solar-wind proton access deep into the near-Moon wake, *Geophys. Res. Lett.*, *36*, L16103, doi:10.1029/2009GL039444
- Nishino, M.N., M. Fujimoto, Y. Saito, S. Yokota, Y. Kasahara, Y. Omura, Y. Goto, K. Hashimoto, A. Kumamoto, T. Ono, H. Tsunakawa, M. Matsushima, F. Takahashi, H. Shibuya, H. Shimizu, and T. Terasawa (2010), Effect of the solar wind proton entry into the deepest lunar wake, *Geophys. Res. Lett.*, *37*, L12106, doi:10.1029/2010GL043948.
- Ogilvie, K. W., J. T. Steinberg, R. J. Fitzenreiter, C. J. Owen, A. J. Lazarus, W. M. Farrell, and R. B. Torbert (1996), Observations of the Lunar Plasma Wake from the WIND Spacecraft on December 27, 1994, *Geophys. Res. Lett.*, *23*, 1255–1258.
- Omura, Y., H. Kojima and H. Matsumoto (1994), Computer Simulation of Electrostatic Solitary Waves: A Nonlinear Model of Broadband Electrostatic Noise, *Geophys. Res. Lett.*, *21*, 2923–2926.
- Omura, Y., H. Matsumoto, T. Miyake and H. Kojima (1996), Electron Beam Instabilities as Generation Mechanism of Electrostatic Solitary Waves in the Magnetotail, *J. Geophys. Res.*, *101*, 2685–2697.
- Omura, Y., H. Kojima, N. Miki, T. Mukai, H. Matsumoto, and R. Anderson (1999), Electrostatic Solitary Waves Carried by Diffused Electron Beams Observed by GEOTAIL Spacecraft, *J. Geophys. Res.*, *104*, 14,627–14,637.
- Ono, T., A. Kumamoto, Y. Yamaguchi, A. Yamaji, T. Kobayashi, Y. Kasahara, and H. Oya (2008), Instrumentation and Observation Target of the Lunar Radar Sounder (LRS) Experiment on-board the SELENE Spacecraft, *Earth, Planets and Space*, *60*, 321–332.
- Saito, Y. et al. (2008), Low energy charged particle measurement by MAP-PACE onboard SELENE, *Earth Planets Space*, *60*, 375–386.
- Shimizu, H., F. Takahashi, N. Horii, A. Matsuoka, M. Matsushima, H. Shibuya, and H. Tsunakawa (2008), Ground calibration of the high-sensitivity SELENE lunar magnetometer LMAG, *Earth Planets Space*, *60*, 353–363.
- Takahashi, F., H. Shimizu, M. Matsushima, H. Shibuya, A. Matsuoka, S. Nakazawa, Y. Iijima, H. Otake, and H. Tsunakawa (2009), In-orbit calibration of the lunar magnetometer onboard SELENE (KAGUYA), *Earth Planets Space*, *61*, 1269–1274.
- Tsunakawa, H., H. Shibuya, F. Takahashi, H. Shimizu, M. Matsushima, A. Matsuoka, S. Nakazawa, H. Otake, Y. Iijima (2010), Lunar magnetic field observation and initial global mapping of lunar magnetic anomalies by MAP-

K. Hashimoto, M. Hashitani, Y. Omura, Research Institute for Sustainable Humanosphere, Kyoto University, Uji, Kyoto 611-0011, Japan. (kozo@rish.kyoto-u.ac.jp)

Y. Kasahara, Information Media Center of Kanazawa University, Kanazawa 920-1192, Japan

T. Ono, Graduate School of Science, Tohoku University, Aoba-ku, Sendai 980-8578, Japan

M. N. Nishino, Y. Saito, and S. Yokota, Institute of Space and Astronautical Science, Japan Aerospace Exploration Agency, 3-1-1 Yoshinodai, Sagami-hara 229-8510, Japan.

M. Matsushima, F. Takahashi, and H. Tsunakawa, Department of Earth and Planetary Sciences, Tokyo Institute of Technology, 2-12-1 Ookayama, Tokyo 152-8551, Japan.

H. Shibuya, Department of Earth and Environmental Sciences, Kumamoto University, Kumamoto 860-8555, Japan.

H. Shimizu, Earthquake Research Institute, University of Tokyo, 1-1 Yayoi, Tokyo 113-0032, Japan.

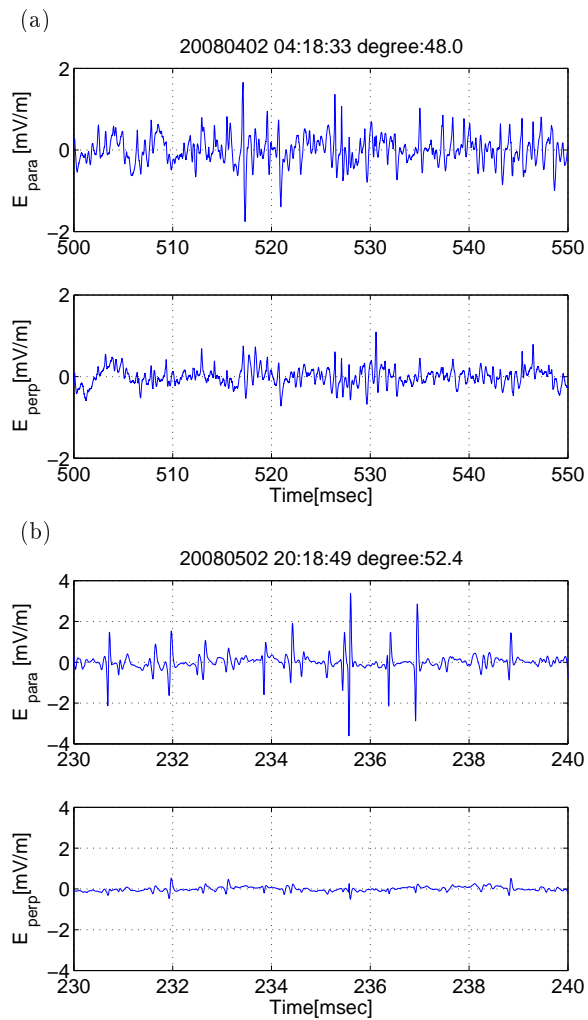


**Figure 1.** Examples of electrostatic solitary waves (ESWs) observed by KAGUYA WFC-L waveform receiver. (a) Type A ESWS observed on April 2, 2008 at 0418 UT in a wake boundary, (b) Type B ESWS observed on May 2, 2008 at 2018 UT above a magnetic anomaly. Electric field components parallel and perpendicular to the local magnetic field are shown in the top and the bottom in each panel, respectively. Following the word, 'degree' in the title, the nadir angle (see the text) is indicated.

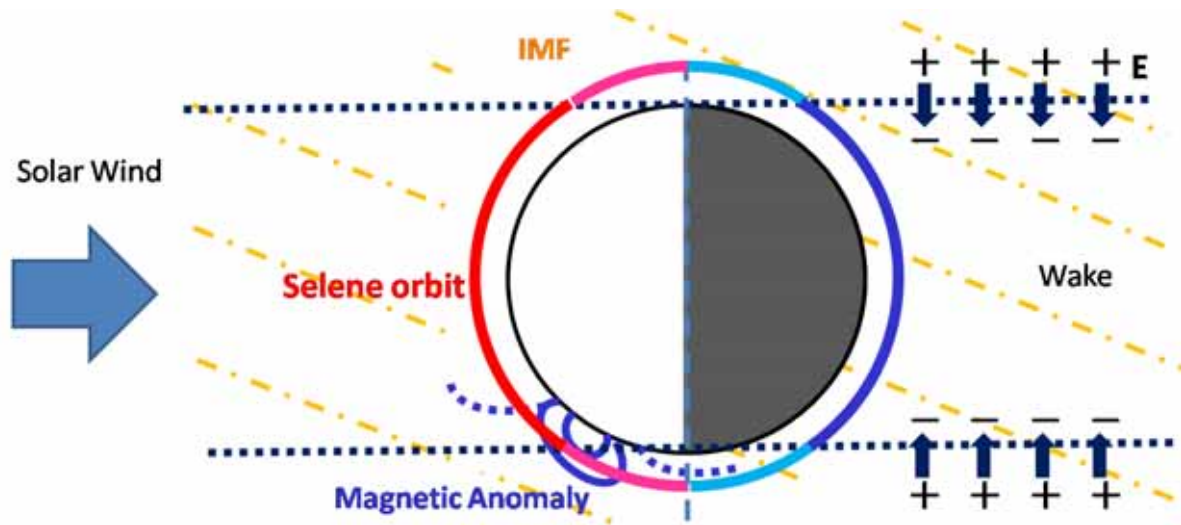


**Figure 2.** Schematic diagram on KAGUYA orbit and four regions defined in the present paper. Circle around the Moon: The KAGUYA orbit. Red: Above the sunlit region. Blue: The wake backside of the Moon. Magenta and cyan: Boundaries facing the Sun and the wake, respectively, just outside of the blue dashed lines which start from the Sun and are tangent to the lunar surface. The yellow dash-dot lines indicate the interplanetary magnetic field.



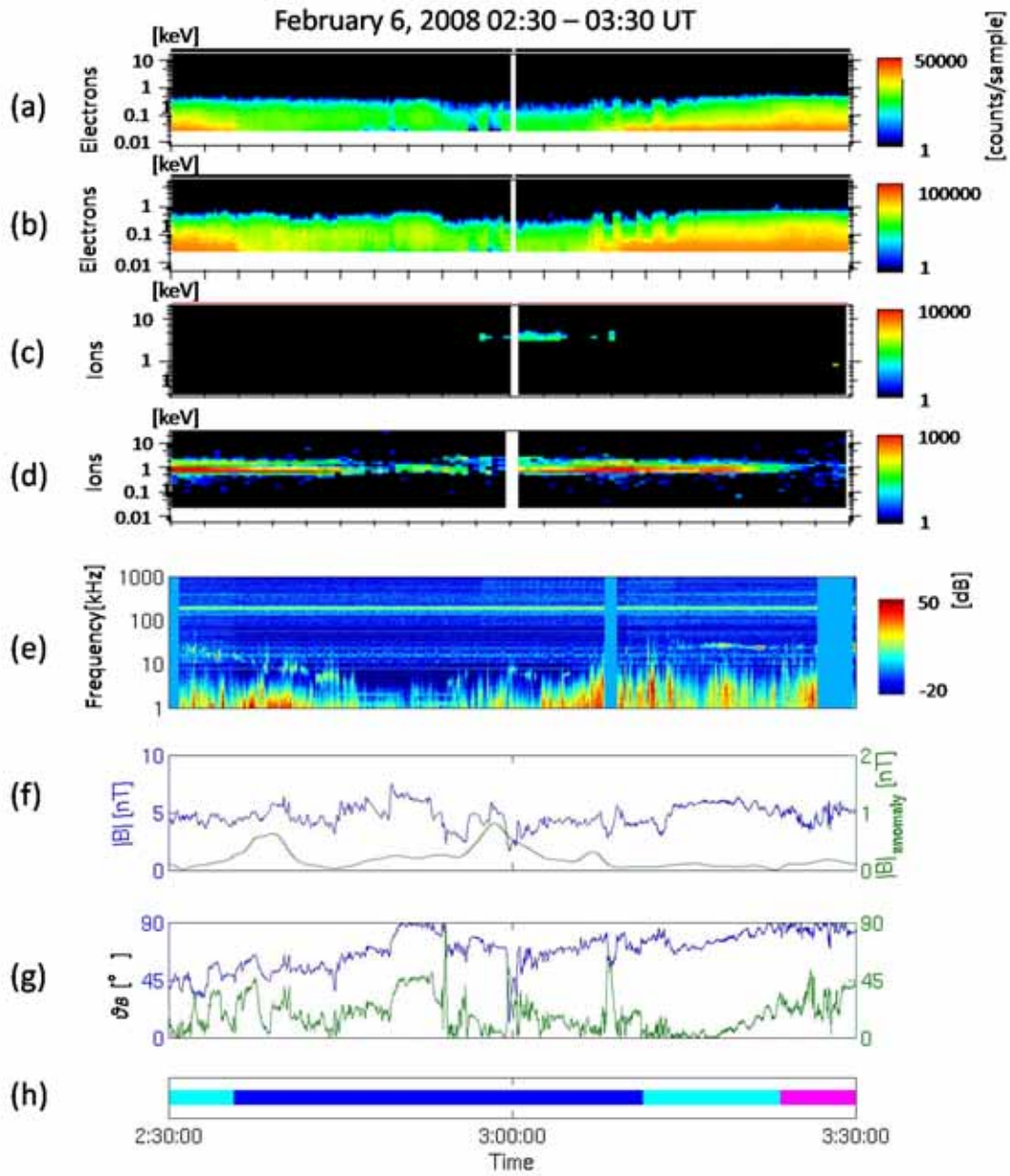


**Figure 3.** Type A ESW. Data of particles by MAP/PACE, wave spectra by WFC-H, and magnetic fields by LMAG observed on February 6, 2008 from 0230 to 0330 UT in a wake boundary. (a) and (b) Energy-time diagrams for electrons toward the Moon by ESA2 and those from the Moon by ESA1, respectively. (c) and (d) E-t diagrams for ions toward the Moon by IEA and those from the Moon by IMA, respectively. (e) Dynamic spectra of an wave electric field from 1kHz to 1MHz. In (f), blue and green lines show intensities of total magnetic field and model magnetic anomaly [Tsunakawa *et al.*, 2010], respectively. The scale of the latter is shown on the right axis. (g) Blue and green lines show the nadir and tail angles (see the text), respectively. (h) Observed zones defined in Figure 2 in colored bars.

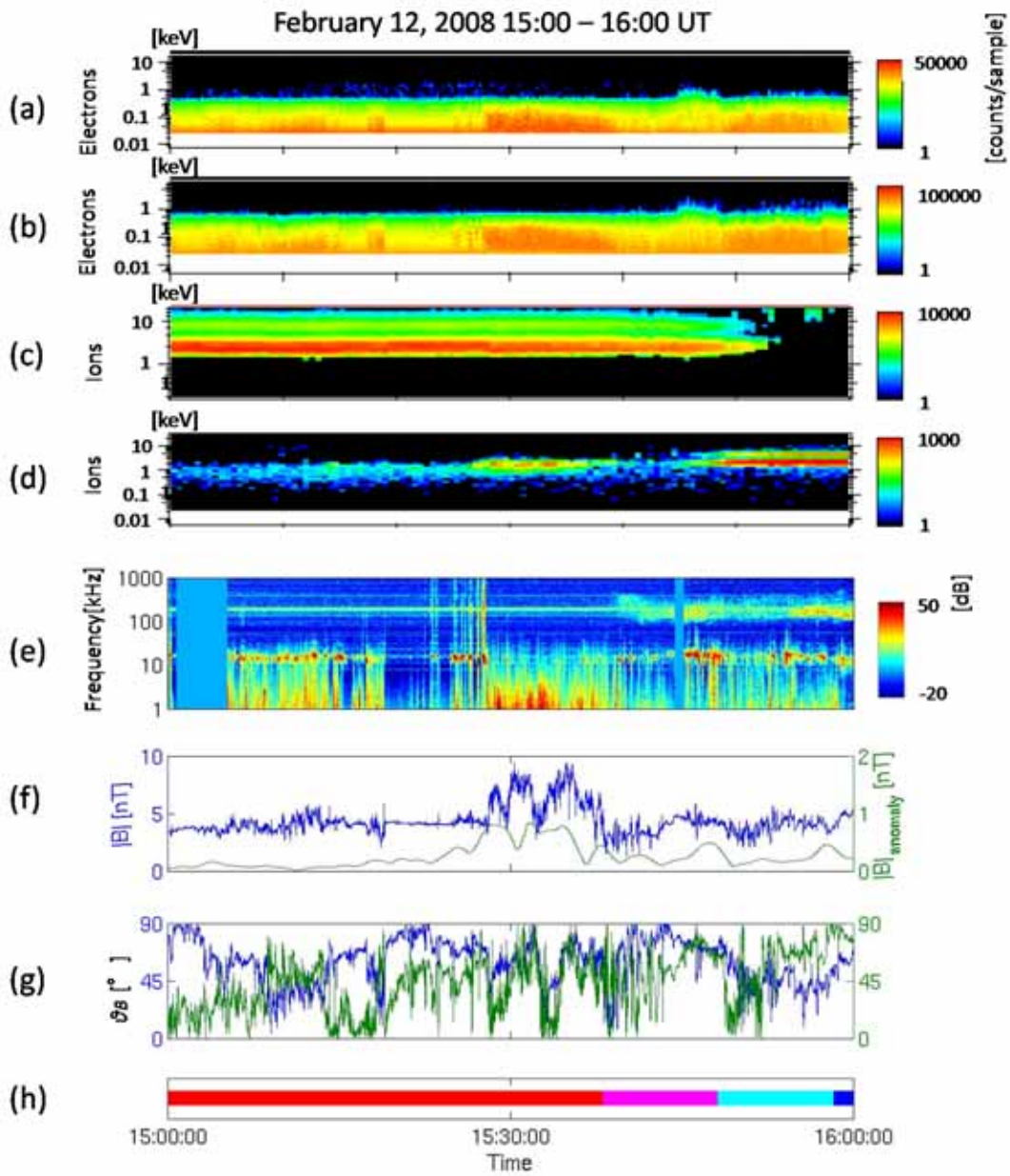


Figure 4. Type B ESW observed on February 12, 2008 from 1500 to 1600 UT above a magnetic anomaly in the solar wind in the same format as Figure 3

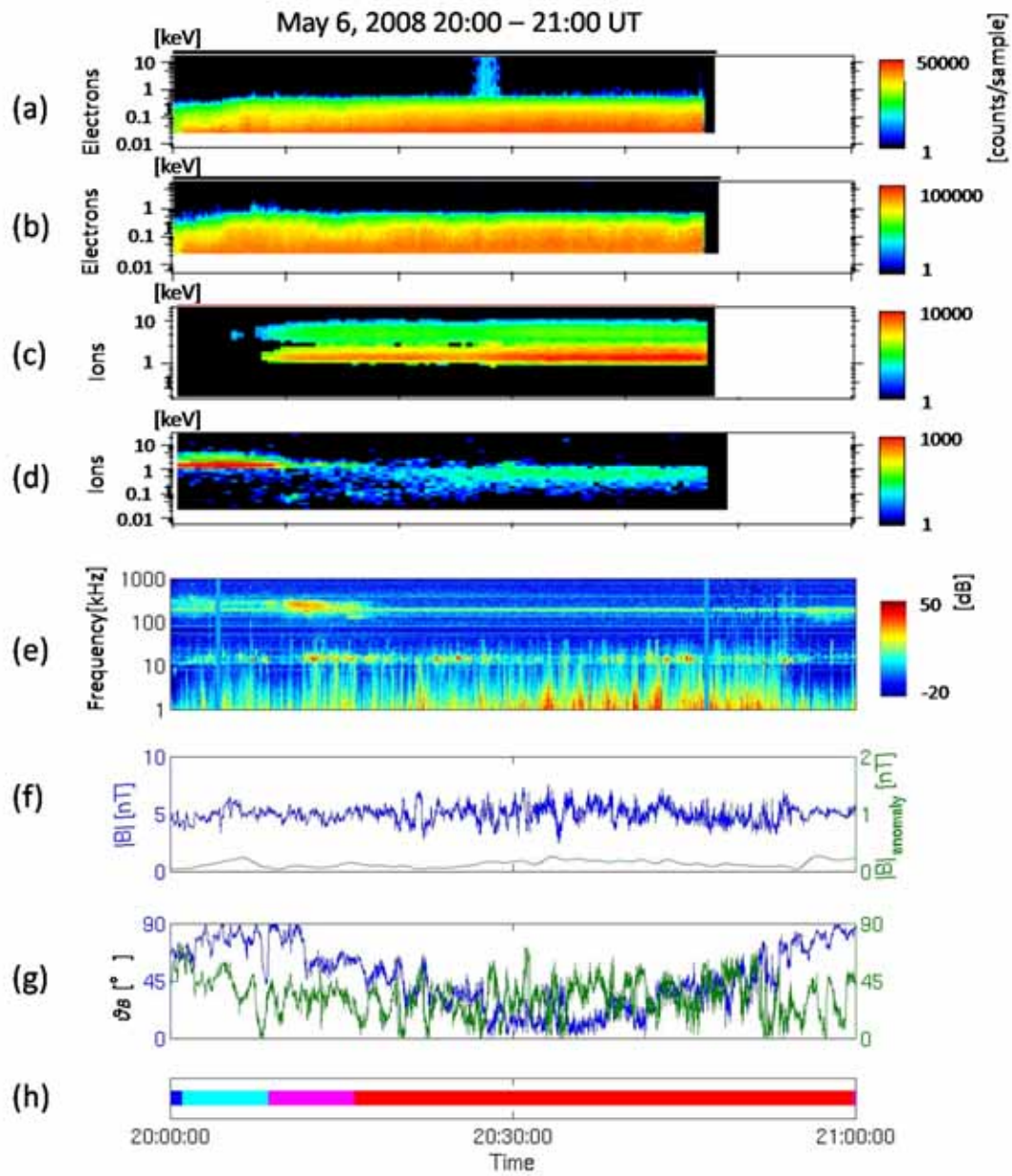


Figure 5. Type C ESW observed on May 6, 2008 from 2000 to 2100 UT in the solar wind in the same format as Figure 3.